Aquat.sci.62 (2000) 105–124
1015-1621/00/020105-20 $ 1.50+0.20/0

Aquatic Sciences

Numerical modeling of thermal stratification in a lake reservoir. Methodology and case study

Marie-Paule Bonnet[1,*], Michel Poulin[1] and Jean Devaux[2]

[1] Ecole de Mines de Paris, CIG 77305 Fontainebleau Cedex, France
[2] Laboratoire de Protistologie, Universite de Clermont II, Aubieres, France

Key words: Numerical modeling, hydrodynamics, lake.

ABSTRACT

A numerical model of the hydrodynamic and thermal structure of an artificial lake was designed and developed as a basis for an ecological water-quality model. It allows the quantification of the vertical mixing processes that govern not only the thermal structure but also the nutrient exchanges, and more generally the distribution of dissolved and particulate matter between the different parts of the lake. The vertical temperature profiles were calculated by solving the one-dimensional heat transfer equation that takes into account the internal heat sources and sinks, advection due to inflow and outflow and the molecular and eddy diffusions. A finite-difference discretization of first-order in time and second-order in space was chosen. The numerical time-step was three hours and layers were one-meter in thickness. These time- and space-scales are well-suited to perform a precise simulation of the different processes occurring over a seasonal period. Moreover, this simulation requires only a reasonable amount of computer time.

This model was used to study an artificial lake, (i.e. a reservoir), located in the high Loire valley (Roanne, France). To precisely identify the physical processes followed with an accurate numerical modeling, on-site data were acquired intensively over three years. Temperatures were monitored hourly at 11 different levels in the three main reaches of the reservoir to study the lake hydrodynamics and thermal behaviour. Meterological measurements were made every 20 minutes. One-year data were used for calibration, whereas the model was validated using the data collected over the other two years.

1 Introduction

In recent years, several studies have been carried out to tackle the problems of water quality deterioration. They were aimed at identifying the leading factors in the determination of lacustrine ecosystems behavior, then at understanding their interactions. Numerical modeling is a good choice as a technique to achieve such a task because it enables one to simultaneously quantify different factors.

* Present address: Laboratoire d'étude des Transferts en Hydrologie et Environnement, BP 53, Domaine universitaire, 38041 Grenoble Cedex 9, France.

When using numerical modeling, first studying the thermal behavior and hydrodynamics in a lake is essential because it allows one to quantify the vertical exchanges governing the vertical distribution of dissolved and particulate matter. This becomes important if the lake is stratified. In such a case the euphotic zone where the phytoplankton grows is essentially a zone of oxygen and organic matter production and of nutrients consumption. On the other hand, organic matter is degraded and oxygen consumed, whereas nutrients are redissolved in deeper layers. Assessing the exchanges between these two areas is important because they influence the trophic organization of the ecosystem. In depth physical description of hydrodynamics, is therefore a necessary prerequisite in the understanding of lacustrine ecosystems as physical and biological processes interact in several ways and at various time- and spatial-scales (Holloway, 1984; Gargett, 1991; Patterson, 1991; Belyaev, 1992; MacIntyre, 1993).

In the last few years, several one-dimensional models have been developed. They can be classified into two main categories:

– The models based on turbulence closure schemes where the rates for vertical transport are related to the turbulent kinetic energy. Typical models of this category are DYRESM (Imberger and Patterson, 1981; Hamilton and Schladow, 1997), the models proposed by Gaspar et al. (1990) and Kantha and Clayson (1994) or the new release of AQUASIM (Goudsmit et al., 1996). All these models can simulate transport processes quite accurately but their development is more difficult and requires more input data than those of the second group.
– Advective-diffusive models which describe vertical transport by simple formulations or preset rates. MINLAKE (Riley and Heinz, 1988), LIMNMOD (Karagounis et al., 1993) and AQUASIM (Reichert, 1994) constitute the main typical models in this category. They are easily developed, require less input data than the former ones, but they usually have a low temporal resolution.

The model presented here belongs to the second category. The formulations of the eddy diffusion coefficients follow the lake structure, i.e., the epilimnion where wind induced mixing predominates, the metalimnion and the hypolimnion where stability effects predominate. As the model was designed for studying a reservoir, it also took into account variations of the surface level and several withdrawal depths. Comparisons with an extensive database allowed us to check the robustness of the conceptual scheme of our model. This model can describe the seasonal and daily variations of the thermal strucutre while consuming a reasonable amount of computer time. In addition, it gives a good representation of large-scale vertical exchanges.

This work is the first part of a multidisciplinary study focused on the biological behavior of a water reservoir located on the river Loire.

2 Site description and data acquisition

2.1 The Study Site

This study was carried out in the Villerest reservoir ($-4.3E$, $43.2°N$) built by EPALA, the Agency in charge of managing the Loire river with its tributaries. The

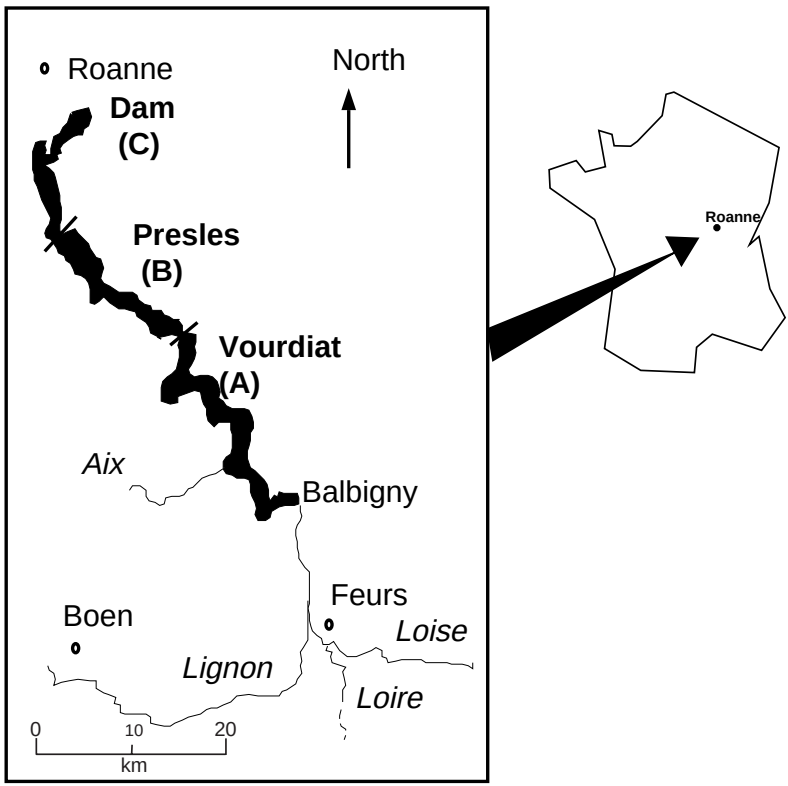

Figure 1. Situation map

deterioration of the water quality over the last ten years was very fast and accompanied by algal blooms dominated by the cyanobacteria *Microcystis aeruginosa* (Aleya et al., 1994). Data were collected from April 1990 to December 1992.

The location of the site is depicted in Figure 1. Its morphometric characteristics are listed in Table 1.

This reservoir was filled in 1984. It has been designed to regulate the Loire flow, and thus, the elevation of its surface level during our study varied by ± 15 m. Its maximum depth is 45 m. Generally, the withdrawal period starts in July and extends to the end of September.

Table 1. Morphometric characteristics of Villerest reservoir

Maximum depth	45 m
Length	35 km
Maximum width	900 m
Lake surface (elevation 315 m)	$700 \cdot 10^4$ m^2
Average volume	$62 \cdot 10^6$ m^3
Average depth	18 m

Table 2. Meteorological data recording near the dam

Sensor	Accuracy
Wind direction	± 5°
Wind speed 10 and 6 m above the surface	± 20 cm · s^{-1}
Dry and moist temperature	± 0.25 °C
Incident solar radiation (0.3 to 2.5 μm)	± 20 W · m^{-2}

Within April 1990 and December 1992 the reservoir behavior was nearly the same: In springtime, the residence time was relatively short (less than 3 months) and the water quality of the reservoir was strongly influenced by the inflow. In summertime, as inflow decreased, the residence time increased and the water quality of the reservoir was less influenced by the river.

2.2 Data acquisition

Morphometric characteristics can cause thermal variations between upstream and downstream areas. Temperatures were measured in the three principal reaches of the reservoir: the first station, *C*, was near the dam, the second one, *B*, and the third one, *A*, were 12 km and 25 km respectively from the dam. Each measurement was performed and recorded at 11 different levels on a 1-hour time step using a Model-7 temperature profile recorder (Aanderaa instrument). The 45 m-long thermistor string was placed at station *C* with a 4.5 m-distance between neighbouring sensors. A ballast maintained the string vertical despite surface level variations. The river temperature was measured at the entrance of the reservoir on a 1-hour time step.

A meteorological station was located on the bank near the *C* station, and the parameters listed in Table 2 were recorded on a 20-minute time step. Some other data not available on site were provided to us by a station of the French Meteorological network, i.e. MeteoFrance, located 40 km away from the dam near its entrance. They consisted of cloud cover, dry and wet-bulb temperatures (used to measure atmospheric humidity) and atmospheric pressures. They enabled us to calculate the heat balance between the water and the atmosphere at the surface as indicated in Table 3.

Inflow and outflow data were provided by the Hydrology Department of EPALA that collects all the data dealing with the Loire catchment area. The river flow rate and the surface level elevation were measured every 4 h. These data were required to establish the hydrological budget for the reservoir under study. EPALA provided the calibration curve establishing the relationships between the surface level elevation and area, and the elevation and volume of the reservoir.

Table 3. Equations of the radiative exchanges at the water-atmosphere interface

Short wave radiations $W \cdot m^{-2}$

$\Phi_s = a_1\ \Phi_0 (\sin h)^{b_1}\ (1 - 0.65C^2)$
where h, is the hour angle, C is the cloud cover,
$\Phi_0 = 1390\ W \cdot m^{-2}$ is the solar constant
$a_1 = 0.79$ and $b_1 = 1.15$ are two calibration parameters determined by comparison with the radiometer data

Long wave radiations $W \cdot m^{-2}$

$\Phi_{ra} = \varepsilon_a \sigma_s T_a^4$
where $\varepsilon_a = 0.937 \cdot 10^{-5}\ (1 + kC^2) T_a^2$ is the air emissivity,
T_a, is the absolute air temperature (K), $\sigma_s = 5.67 \cdot 10^{-8}\ W \cdot m^{-2} \cdot K^{-4}$,
is the Stephan-Boltzman constant
C is the cloud cover and $k = 0.17$ is a parameter depending upon the cloud characteristics

$\Phi_{rw} = \varepsilon_w \sigma_s T_w^4$
where $\varepsilon_w = 0.96$, is the water emissivity,
T_w, is the absolute water temperature (K) in the upper layer

Non radiative radiations

Latent heat flux $W \cdot m^{-2}$

$\Phi_e = c_e \rho_a\ (a + bV_2)\ Ł_w (T_w)\ (q_s - q_2)$
$Ł_w (T_w) = (2500.9 - 2.365\ (T_w - 273))\ 10^3$

$$q_s = \frac{0.622\ e_{s0}}{P_a - 0.378\ e_{s0}},\ q_2 = \frac{0.622\ e_2}{P_a - 0.378\ e_2}$$

$$e_{s0} = \exp\left[2.3026\left(\frac{7.5\ T_{surf}}{T_{surf} + 237.3} + 0.7858\right)\right]$$ Magnus Tetens formula

$e_2 = e_{s2} - \Psi P_a\ (T_a - T_{ha})$ (Queney, 1974)

with $\Psi = 7.9 \cdot 10^{-4}$ without ventilation, $\Psi = 6.6 \cdot 10^{-4}$ with ventilation

with the following notations:

ρ_a, is the air density $(kg \cdot m^{-3})$,
c_e, a and b are three calibration parameters (values given in Table 4)
P_a, the atmospheric pressure (mb)
T_{surf}, is the water temperature in the upper layer (°C)
V_2, is the wind speed at 2 m above the surface $(m \cdot s^{-1})$
It is deduced from the measured wind at 6 m above the surface V_6

with the Schmidt formula $V_2 = V_6 \left(\frac{2}{6}\right)^{0.3}$

$L_w (T_w)$, is the latent heat of vaporisation $(J \cdot kg^{-1})$ (Huber and Harleman, 1968)
q_s and q_2, are the specific humidities at saturation and at 2 m above the surface respectively,
e_{s0}, is the vapour pressure at saturation (mb).
e_2, is the vapour pressure two meters above the water surface (mb)
e_{s2}, is the vapour pressure at saturation 2 m above the water surface (mb)
It is given by the Magnus-Tetens formula replacing T_{surf} by the air temperature (°C) measured at 6 m above the water surface.
T_{ha}, is the measured absolute moist air temperature (K)

Sensible heat flux $W \cdot m^{-2}$

$\Phi_{sh} = \rho_a\ (a + bV_2)\ (T_w - T_a)$ (Gaillard, 1981)
using the same notations as above

3 Model description

3.1 Equation solved

The choice of the space and time discretization was a trade-off between the processes to be modelled and the computational expense. First of all, it has been shown (Imberger and Patterson, 1990) that when stratification is established in small to medium lakes, transverse and longitudinal heterogeneities are negligible compared to those in the vertical direction. Over recent years, increased computing power has meant that the representation of increased spatial dimensionality is achievable (Casulli and Cattani, 1994). However, this increase in spatial representation consequently requires more computation time, often placing constraints on the length of simulation runs. Moreover, 2-D and 3-D models obviously require extensive field data in order to validate variations in each spatial dimension. As such, 2-D and 3-D models still generally have a limited role in long-term lake management decisions and strategies (Hamilton et al., 1995). As our physical model was a basis for forecasting water quality over seasonal time period, we therefore chose to develop a one-dimensional vertical model. First, its precision was sufficient to describe the main mixing processes, and second, it used short computer time. Therefore, the basic equation for expressing the temperature T (°C) at the time t and at depth z (z positive in upward direction) can be expressed by:

$$\frac{\partial T}{\partial T} = \frac{1}{A}\frac{\partial}{\partial z}\left[AK(z)\frac{\partial T}{\partial z}\right] - \frac{1}{A}\frac{\partial \omega T}{\partial z} + S \tag{1}$$

with

$$S = \frac{\partial}{\partial z}\left[\frac{R_s}{\rho C_p}\right] + QT_r \tag{2}$$

where T is the temperature (°C), $K(z)$ is the vertical diffusion coefficient ($m^2 \cdot s^{-1}$), w is the vertical advective flow due to in- and outflow ($m^3 \cdot s^{-1}$), A is the cross sectional area (m^2), S is the source/sink term (°C · s^{-1}), R_s the source term due to surface-atmospheric exchanges (W · m^2, see paragraph 3.3), QT_r denotes the in- and output of heat in (e.g. river) or from (outflow) the lake (°C · s^{-1}), ρ is the water density (kg · m^{-3}) and C_p is the specific heat (J · kg^{-1} · °C^{-1}).

For each layer, the term QT_r is given by:

$$QT_r = \frac{q_{in}T_{riv} - q_{out}T}{V} \tag{3}$$

where T, V, q_{in} and q_{out} are respectively the temperature (°C), the volume (m^3), the in- and outflow rates ($m^3 \cdot s^{-1}$) of the considered layer and T_{riv} is the river temperature (°C).

3.2 Processes taken into account

Vertical exchanges create the thermal structures of the lake as most of the heat transfer takes place at the lake surface, then progressively affects all the layers downwards. The model discussed here took into account the main mixing processes: the advection related to throughflows, the eddy diffusion induced by wind and internal seiches, the mixing due to surface waves and free convection. In addition, the model presented here took into account the contribution of a tributary stream and the influence of withdrawals at different levels.

3.2.1 Advection

Advective fluxes are related to the inflow and outflow. In case of heavy throughflows advection can greatly affect the thermal stratification.

The level of the river intrusion depends on density vertical structure and entrainment. In the model, the equal-density level is used to determine where the river enters (Giovanoli, 1990). The entrainment of the water mass is simulated by a vertical distribution of the velocity field. According to Ryan and Harleman (1971) and Lafforgue (1990), it is assumed that the velocity distribution is Gaussian with a standard deviation that depends on both the rate of inflow and the stability of the water column:

$$\sigma_{in} = \sigma_r \frac{1}{\Delta T(z_{in})} \frac{tq_{in}}{tq_{mean}} \tag{4}$$

where σ_{in} is the standard deviation of the Gaussian distribution, tq_{in} is the rate of the river flow ($m^3 \cdot s^{-1}$), tq_{mean} is the one-year mean rate of the river flow which is used here to normalize the distribution ($m^3 \cdot s^{-1}$), $\Delta T(z_{in})$ is the temperature gradient at the level of the river entrance ($°C \cdot m^{-1}$), and σ_r is a calibration parameter ($m \cdot °C^{-1}$) (mentioned in Table 4). However, when the river waters enter an area with a high density gradient (Fig. 2) the model uses an asymmetrical distribution to take into account the density gradient on the two sides of the entrance level. Standard deviations of the two Gaussian branches are deduced from the density grdient computed on either side of the entrance level in a similar way as indicated in Equation 4.

The outflow velocity distribution was assumed to be uniform for the layers facing the outlet area. Moreover, the outflow was assumed to come from both sides of the outlet with a Gaussian distribution centered on the top- and bottom-levels of the outlet respectively. Two calibration parameters p_t and p_l, (mentioned in Table 4) gave the percentage of outflow from each side of the outlet.

As, in a reservoir, withdrawals may occur at several levels, this phenomenon was introduced into the numerical model. The number of outlets, their individual level and outflow rates were entered as input data. The velocity distribution was calculated for each outlet as previously indicated and the velocity profiles were superimposed.

The vertical velocities were calculated on stating that the mass balance equation was satisfied at each level. The model convention was to set to zero the inflow across the bottom and to calculate the velocity upwards from bottom.

Table 4. Expression of the eddy diffusion coefficients

Parameter	Assigned value	Units
Calibration of heat exchanges		
a	1.17 (calibrated)	$(m \cdot s^{-1})$
b	1.15 (calibrated)	(–)
c_e	$3.46 \cdot 10^{-3}$ (calibrated)	(–)
Calibration of dispersion coefficients		
δ	0.06 (calibrated)	$(s^{1/2})$
C_{10}	$1.3 \cdot 10^{-3}$ (fixed)	(–)
σ	7 (calibrated)	(–)
p_1	0.14 (calibrated)	(–)
α	0.15 (calibrated)	(–)
p_2	0.06 (calibrated)	(–)
Calibration of inflows-outflows velocities		
σ_t	0.6 (calibrated)	(–)
p_t	0.014 (calibrated)	(–)
p_l	0.13 (calibrated)	(–)

3.2.2 Dispersion

In the present work the eddy diffusion coefficient was formulated from the lake structure proposed by both Tassin (1986) and Vinçon-Leite (1991) (Table 5): the epilimnion, where the mixing due to the wind is very efficient, the metalimnion and hypolimnion, where the effects of wind are reduced and the stability effects greater. Therefore in the epilimnion, as the lake is stratified, the coefficient $K(z)$ is related to the value of the coefficient under neutral conditions $K_0(z)$ (Simons, 1981) whereas in the metalimnion and the hypolimnion $K(z)$ expressions are related to the stability N^2 (Jassby and Powell, 1975). Moreover, as in the hypolimnion internal waves may induce more turbulent mixing, a correction factor is added (Vinçon-Leite, 1991). It is bounded by a maximum value of $5 \cdot 10^{-3}$ $m^2 \cdot s^{-1}$.

The molecular diffusion was indirectly taken into account by bounding the eddy diffusion coefficient with the lower bound at $1.2 \cdot 10^{-7}$ $m^2 \cdot s^{-1}$ (Henderson-Sellers, 1984). We neglected here the temperature dependence of the molecular diffusion.

3.2.3 Mixing due to waves and free convection

Assuming the fetch is constant, the wave-mixed depth was calculated with the method proposed by Smith (1979). The eddy diffusion coefficient in the wave-mixed layer was set to 5.10^{-3} $m^2 \cdot s^{-1}$ as a maximum.

Convective mixing takes place when density instability appears as a consequence of a temperature decrease in the upper layer. In our study, the water stability was tested at the end of each time step. When required, mixing was processed downwards until stability established.

Table 5. Calibration parameters and assigned values

Diffusivity in the epilimnion $m^2 \cdot s^{-1}$

Homothermic lake

The expression is deduced from Simons (1981):

$$K_0(z) = (\tfrac{5}{4}\,\delta)^2\, \overset{*}{\omega}{}_s^2 \exp \frac{z - Z_s}{(\tfrac{5}{2}\,\delta)\frac{\overset{*}{\omega}{}_s}{f}}$$

where $\overset{*}{\omega}_s = \sqrt{\frac{\tau}{\rho_w}}$ is the shear velocity at the surface ($m \cdot s^{-1}$),

where $\tau = \rho_a C_{10} V_{10}^2$ is the shear stress at the surface
Z_s is the surface elevation, $\delta \sim 0.1$ is a constant of proportionality and f is the Coriolis parameter
C_{10} is the drag coefficient 10 m above the surface and
V_{10} is the wind speed at the same elevation

Stratified lake

As suggested in Henderson-Seller (1984)
$K(z) = K_0(z)\,(1 + \sigma R_i)^{-p_1}$
where R_i is the Richardson number, σ and p_1 are two calibration parameters (values given in Table 4) such that $(1 + \sigma R_i)^{-p_1} \to 1$ when $R_i \to 0$ and
$(1 + \sigma R_i)^{-p_1} \to 0$ when $R_i \to \infty$

Diffusivity in the metalimnion $m^2 \cdot s^{-1}$

$$K_m(z) = \alpha K_{th} \left(\frac{N_{th}^2}{N^2(z)} \right)^{p_2}$$

where K_{th} and N_{th}^2 are the dispersion coefficient and the stability at the thermocline elevation, α and p_2 are two calibration parameters (values given in Table 4)

Diffusivity in the hypolimnion $m^2 \cdot s^{-1}$

$$K_m(z) = \frac{z}{Z_m} K_m \left(\frac{N_m^2}{N^2(z)} \right)$$

with K_m and N_m^2 the dispersion coefficient and the stability at the base of the metalimnion elevation Z_m.
The correction factor $\frac{z}{Z_m}$ is introduced as described in Vinçon-Leïte (1991) to take into account the influence of internal waves

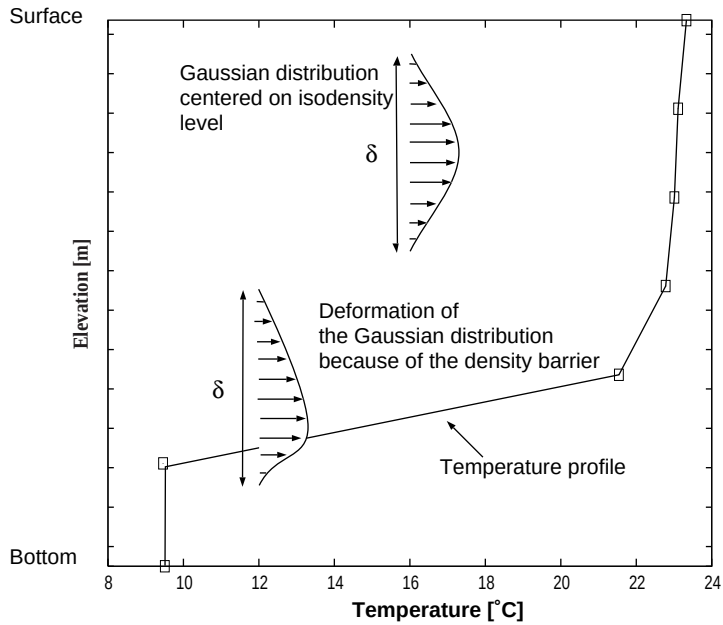

Figure 2. Schematic inflow velocity distribution: an asymmetrical distribution is used to take into account the density gradient on both sides of the entrance level

3.3 Surface Boundary conditions

The heat balance, Φ_{tot}, at the surface of the lake can be summarised as:

$$\Phi_{tot} = (1 - albedo)\,\Phi_s + \Phi_{ra} - \Phi_{rw} - \Phi_e - \Phi_{sh} \tag{5}$$

where, Φ_s is the short wave radiation, Φ_{ra} is the atmospheric radiation, Φ_{rw} is the back radiation, Φ_e and Φ_{sh} are the latent heat flux and sensible heat flux respectively. A mean value of 6% was adopted for the *albedo*. Units for radiations and fluxes are $W \cdot m^{-2}$. Most of the formulations used here for the different terms come from the TVA technical report (1972) and are listed in Table 3.

About 50% of the incoming shortwave radiation is kept in the upper few centimeters of the water column. The remaining fraction penetrates the water column in accordance with Beer's law (Octavio et al., 1977). The extinction coefficient $\eta\,(m^{-1})$ used here was estimated from the Secchi disk data, Z_s (m) and the PAR[1] measured on site. A linear regression analysis over a set of 30 pairs (η, Z_s) led to:

$$\eta = \frac{1.66}{Z_s^{0.77}} \tag{6}$$

[1] The PAR is the photosynthetic active radiation (0.3 to 400 μm).

which is in good agreement with the regression previously established by Garnier (1984).

Finally, R_s in equation 2 is expressed by:

$R_s = \Phi_{tot}$ for the top layer

$R_s = 0.5 \cdot (1 - albedo)\Phi_s \exp(-\eta z)$ below (7)

3.4 Numerical method

The lake was described by a system of 1-m thick horizontal slices, each of them assumed to be homogeneous. We chose a 3-hour time step that allowed us to describe daily variations of the thermal structure.

The model allowed variations in the lake level through variations of the top layer thickness. Below a lower limit of 0.5 m as suggested by Ryan and Harleman (1971), the layer is suppressed. The temperature in the new top layer is expressed as:

$$T_N^{n+1} = \frac{V_N^n T_N^n + V_{N-1}^n T_{N-1}^n}{V_N^n + V_{N-1}^n} \tag{8}$$

where the superscript n refers to the time step, the subscrit N refers to the surface layer, and V is the layer volume (m^3).

When the thickness was larger than 1.5 m, a new layer, characterized by the same temperature as the surface temperature on the previous time step, was introduced into the model. To limit numerical instabilities we stated that the variations in volume of the top slice must not exceed 10% per time step (Lafforgue, 1990). If a greater variation occured, the time step was automatically reduced.

A first-order implicit scheme in time was adopted. The space discretization was done with a second-order finite difference based on quadratic upstream interpolation (Quick method) (Leonard, 1979). The iterative computation usually reached the convergence criteria (10^{-6}) after 3 iterations. The computing time of the model was quite short. A 148-day simulation with 46 slices took only two minutes on a Spark 10.

3.5 Input data and model outputs

Our modeling required the following input data: the meteorological parameters (i.e. dry and moist temperatures, cloud cover, wind speed and, when measured, direct solar radiation), river temperature, lake morphometry, and the level-surface relationship. In addition to temperatures, the model outputs were the advective fluxes, the eddy diffusion coefficient at each level, and the well-mixed depth by free convection. The main terms of the heat balance at the surface and the depth of the euphotic zone were also calculated.

4 Model calibration and validation

We noticed only small changes in the temperature from upstream to downstream. When the vertical stratification was well established, isotherms were nearly horizontal and we could not identify internal waves. We chose to calibrate the model using the data collected between April and September 1991 at station *C* where the reservoir was the deepest. This corresponded to the most complete set of data. The model was validated using the sets of data gathered at the same period of years 1990 and 1992. The numerous data acquired in our database enabled us to carry out a precise calibration and a reliable validation of the model used.

4.1 Model calibration

We noted in Section 3 that the model had to be calibrated. Some terms depend on the geographical location of the lake, others on the lake morphology. Calibration was made by trial and error and by the conjugate gradient method. The latter is well suited to linear problems. We verified that the variations of the objective function (mean square function) that had to be minimized were smooth enough to be linearized. A sensitivity analysis was performed. It showed that the most sensitive parameter was the coefficient c_e that calibrates the evaporation term. The parameter values are listed in Table 4.

4.2 Results

Figure 3 illustrates the variations of heat flux determined from measured and simulated temperatures:

$$E_{\text{cal}} = \frac{1}{A_{\text{surf}}\,\Delta t} \sum_{i=1,N} \rho_{\text{i}}\, C_{\text{p}} V_{\text{i}}\, T_{\text{i, cal}} \tag{9}$$

$$E_{\text{mes}} = \frac{1}{A_{\text{surf}}\,\Delta t} \sum_{i=1,N} \rho_{\text{i}}\, C_{\text{p}} V_{\text{i}}\, T_{\text{i, mes}} \tag{10}$$

where, N is the number of measurement points in the vertical direction, A_{surf} is the lake area (m^2), Δt is the time step (s), ρ_{i} is the water density ($kg \cdot m^{-3}$), C_{p} is the caloric capacity ($J \cdot kg^{-1} \cdot °C^{-1}$), $T_{\text{i, cal}}$ and $T_{\text{i, mes}}$ are respectively the calculated and measured temperatures (°C).

The largest discrepancy between the two plots occured at the beginning of the simulation period (mid-April). It shows that the calculated temperatures were too low, indicating that the heat balance at this time was not very well estimated.

Figure 4 shows the evolution versus time of the measured and simulated temperatures at each level. The temperature was drawn with a grey-scale. The map at the top based on the measured temperatures, shows clearly the incipient stratification

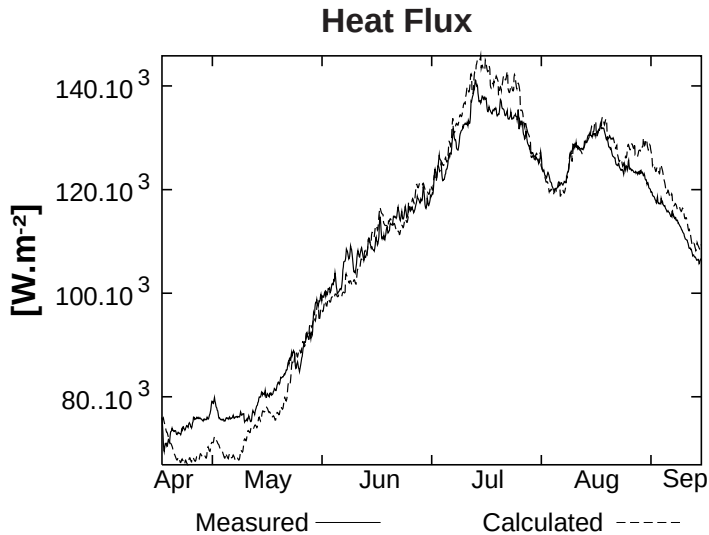

Figure 3. Heat content calculated from measured and computed temperatures

in the reservoir. The thermal stratification in lake Villerest is typical of a dimictic lake in a temperate area. The lake surface temperature increased in mid-April when the net energy flux became positive. From April to June, there was a succession of shallow thermoclines which disappeared rapidly by mixing. The thermocline was very well established in July when heat was received at a rate higher than the rate of transfer to deeper layers. Moreover, the thermocline depth increased rapidly. Because of the closeness of this station to the dam, the vertical temperature profiles were strongly influenced by the withdrawal rates. The thermocline deepened until the next autumn overturn.

With a mean square error of 0.57 °C between the simulated and measured temperatures, one can consider that our model correctly simulated the lake warm-up and the vertical distribution of the temperature. This means that the heat balance at the surface and the transport processes are quite well estimated, large discrepancies being related to times when temperature gradient was large.

Validation consists of testing the model under other meteorological and hydrological conditions. As previously indicated the model was validated using data collected in 1990 and 1992. The results presented here only concern the year 1992. Unfortunately, these data were less numerous than those of 1991, so they sometimes dealt only with the first 20 meters. Figure 5 presents some vertical thermal profiles. The end of spring 1992 was very rainy so there was a flood and the input flow rate was high. Therefore, the management of the reservoir was very different in 1992, the volume variations during the summer were less important. The flood that occurred in mid-June induced a thermal destratification by warming deeper layers. Despite these very different hydrological conditions, the model fitted well the data.

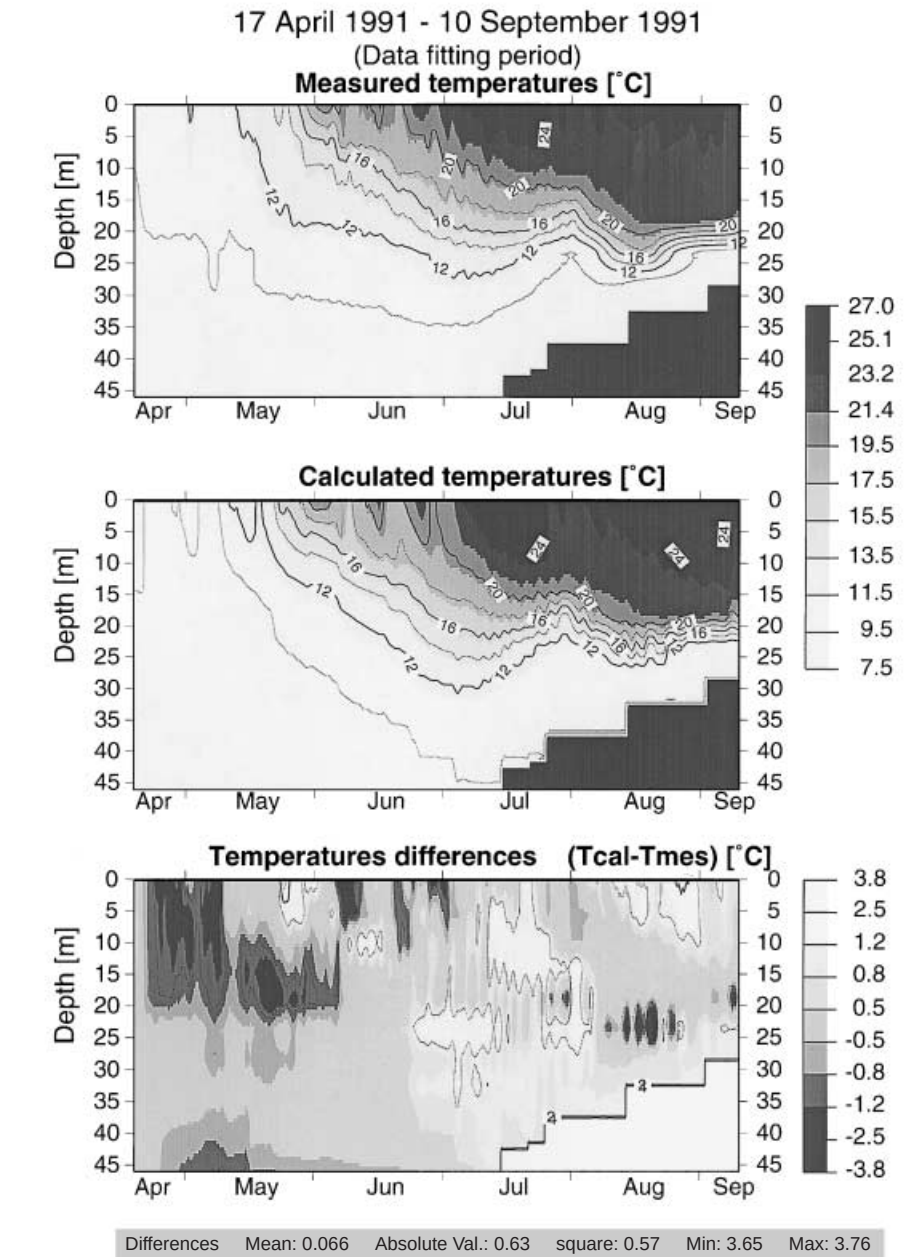

Figure 4. Time evolution of the temperature. The lower the temperature is, the clearer the grey is. The top map is obtained with the measured temperature, the middle one with the calculated one. The bottom one depicts the residues $T_{cal} - T_{mes}$

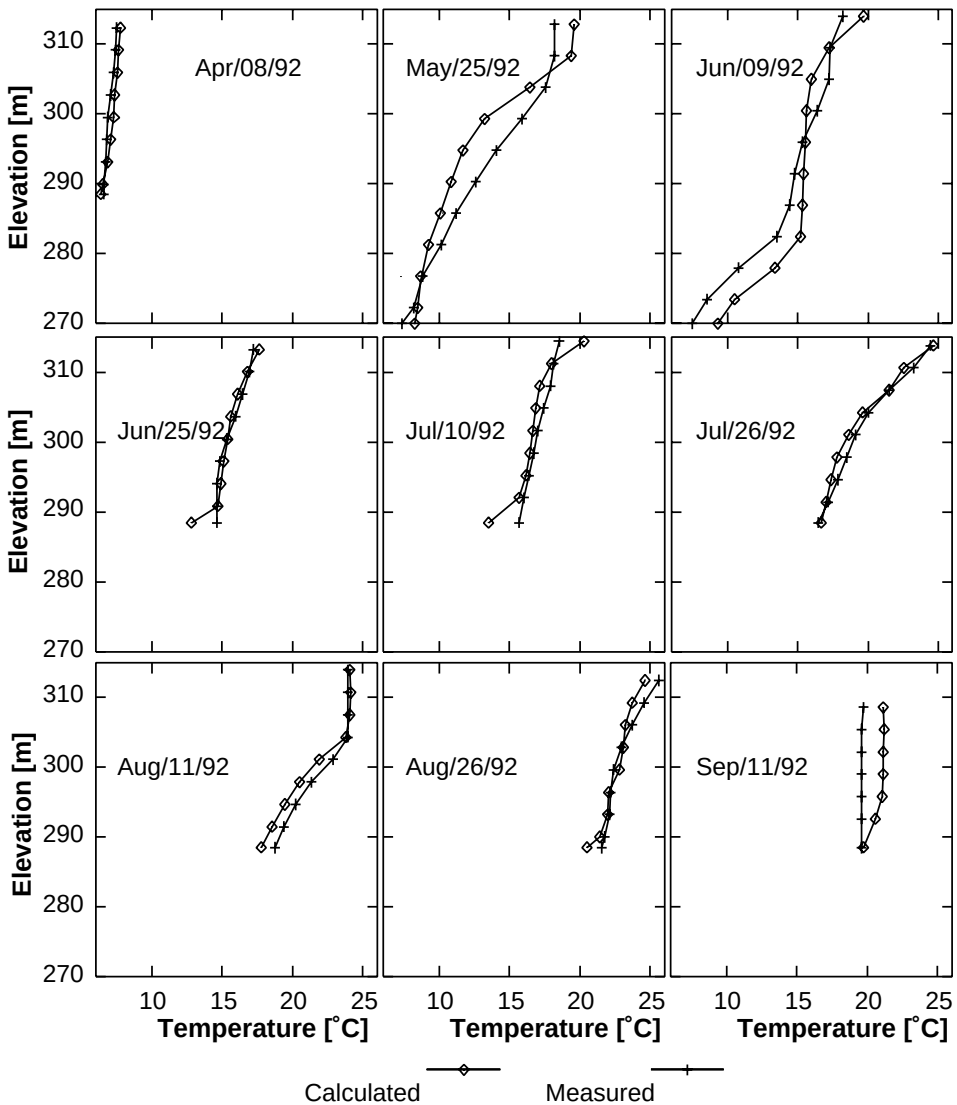

Figure 5. Validation for 1992: vertical temperature profiles. Mostly, only the temperature for the first 20 m is measured

5 Application of the model: Impact of the withdrawal level

One of the major aims of our study was to better understand which factors controlled the water quality in the reservoir and, if possible, to propose some solutions as a help to restore the quality of the water. The model allowed us to simulate some hypothetical scenarios useful for choosing which decisions to make. Our purpose

was to test the impact of the outlet level since the Villerest dam is equipped with outlets at different elevations. At the present time the procedure applied by EPALA consists of withdrawing water from the upper outlet (20 m above the bottom) from May 1st to August 1st and from the lower one (10 m above the bottom) the rest of the time. We wanted to see the impact on the thermal structure of using only the lower outlet and what vertical mixing would be induced. Our simulation covered the same period of study, from April to September 1991. The resulting vertical thermal profiles are depicted in Figure 6.

In the vicinity of the dam, the vertical thermal structure clearly depends on the outlet level. If the lower outlet is used in summer the thermocline becomes deeper. The surface temperature does not change but the bottom water is warmer. The vertical mixing at the bottom of the euphotic zone is not or only slightly modified. In general, the differences in the thermal structure occur at depths greater than that of the base of the euphotic zone. We studied the eddy diffusion values and the vertical advective fluxes at depths of 10 and 20 m. The greatest differences between the two management procedures are found in the advective fluxes shown in Figure 7.

As illustrated in this figure, at 10 m the advective fluxes are weaker when only the deeper outlet is used. At 20 m, they are often in the opposite direction, they go downwards if the deeper outlet is used. In the latter case, from the beginning of July throughout the rest of the period, the advective fluxes are very weak. However, in the same period, they are directed upwards and relatively strong if the upper outlet is used. This leads to an earlier isolation of the layers above 20 m of depth when the lower outlet is used all the time.

6 Conclusion

This study was aimed at building a numerical model of the thermal structure of a reservoir to constitute a good basis for an ecological model to survey water quality.

The model described here was based on the solution of the advective-diffusive heat transport equation by finite differences. A three-hour time step and one-meter space step allowed us to quantify the large-scale vertical exchanges in the reservoir and was well suited to study the seasonal behavior of the lake using a reasonable amount of computing time.

The parameters of the model were calibrated with the most numerous data to ensure a precise calibration. The validation of the model was then successful for two additionnal years, which ensures a reasonable predictability making the numerical model useful in water management for simulating hypothetical scenarios. Our results showed that the location of the withdrawal point determined the location of the thermocline, at least for the closest station to the dam. The deeper the withdrawal point is, the deeper the thermocline is.

Coupling this model with a model describing biological and chemical processes will enable us to test the impact of selective withdrawal on the ecosystem behavior, especially on the phytoplanktonic succession. The oxygen and temperature impacts downstream of such selective withdrawals will have to be studied. The Loire Valley authority will then be in a position to choose the most ecologically-sound management of this recently constructed dam.

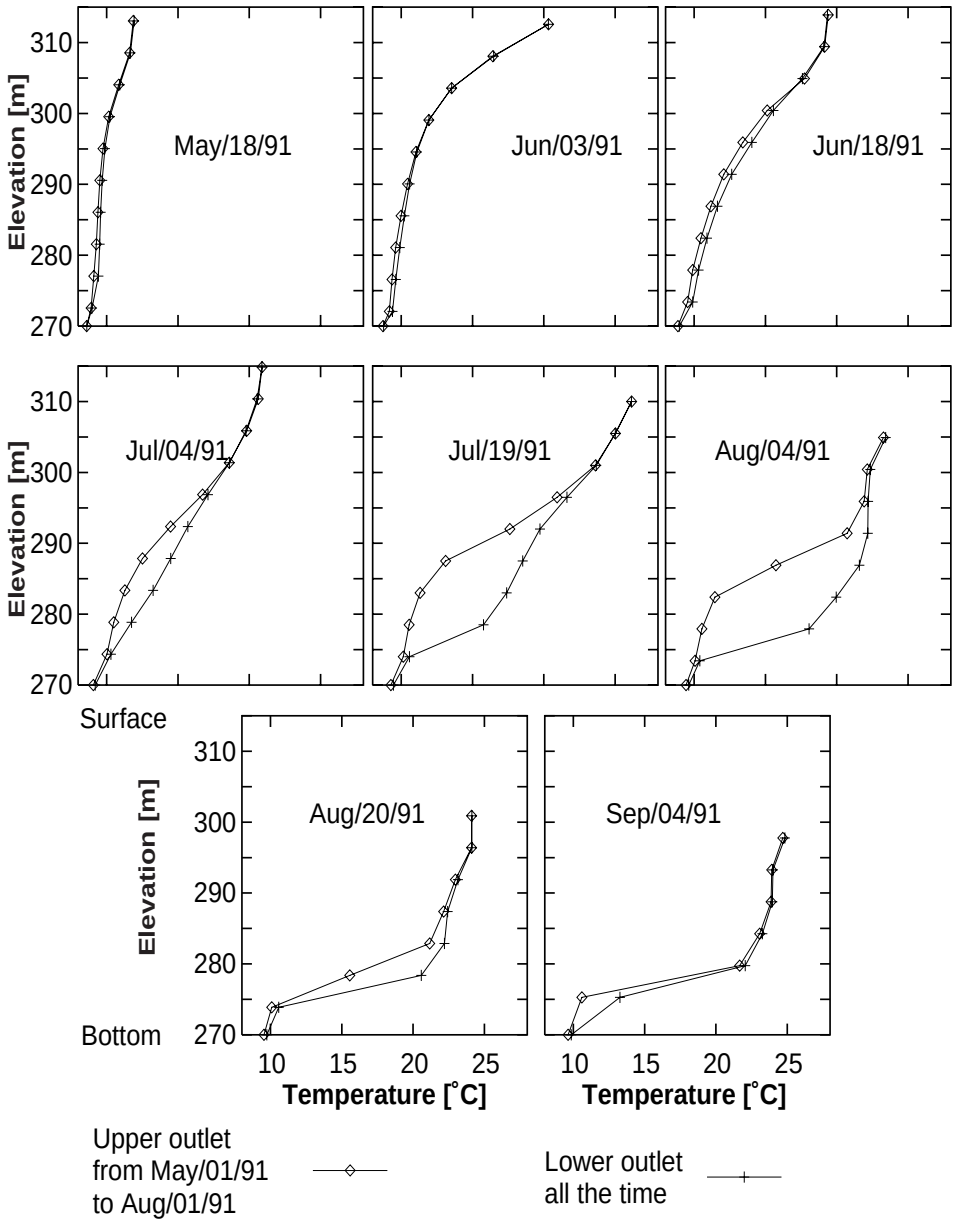

Figure 6. Thermal vertical structure depending on whether the deeper outlet is used all the time or if the upper outlet is used from May to August 1st

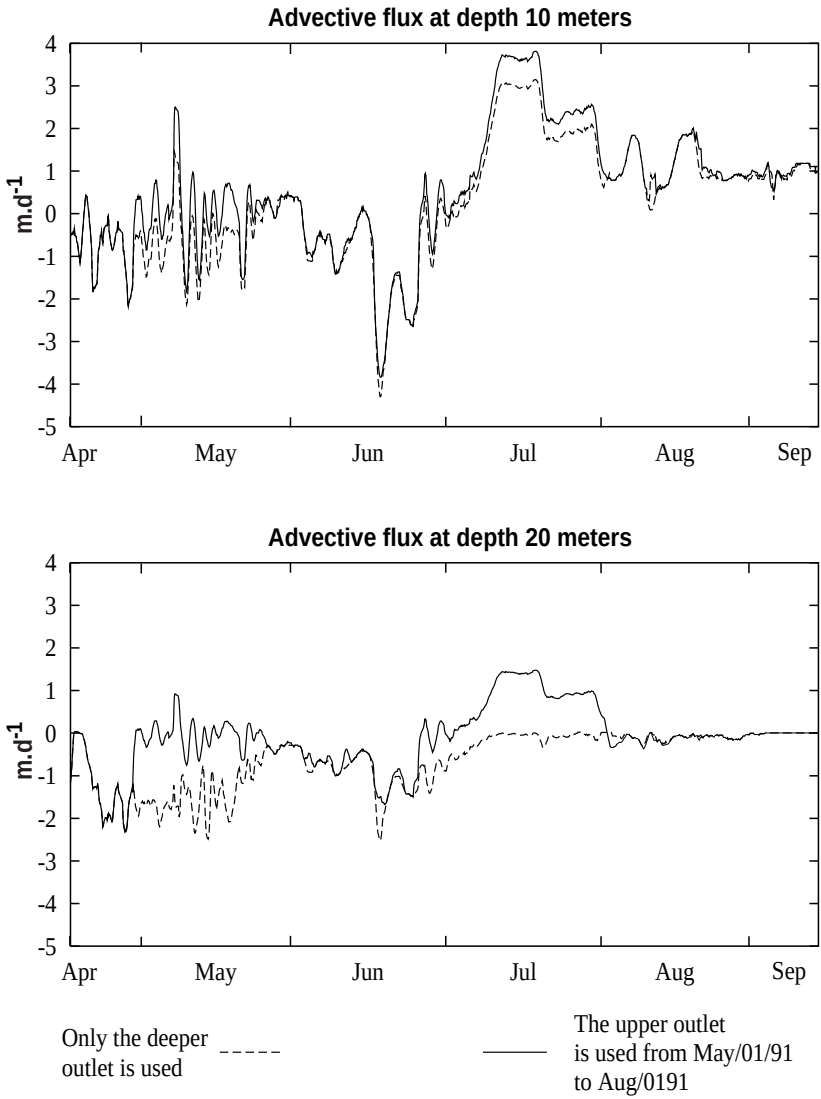

Figure 7. Impact of the outlet location: Advective fluxes at 10 and 20 meters

ACKNOWLEDGEMENTS

The study was founded by EPALA (Agency managing the river Loire and its tributaries). The authors wish to thank Bruno Tassin for helpful discussions and all the people from the Protistology department of the University of Clermont-Ferrand who have helped them with the data collection. They also thank the MeteoFrance station which provided them with very useful data. The writers gratefully acknowledge the two anonymous reviewers for their valuable suggestions and advices. They also thank Marie-Paule Friocourt and Cristina Lumpkin for their careful revision of the English manuscript.

REFERENCES

Aleya L., F. Desmoles, M. Michard, M.P. Bonnet and J. Devaux, 1994. The deterministic factors of the *Microcystis aeruginosae* blooms over a biyearly survey in the hypereutrophic reservoir of Villerest (Roanne, France). Arch. Hydrobiol. 120: 489–515.

Belyaev, V., 1992. Modelling the influence of turbulence on phytoplankton photosynthesis. Ecological Modelling 60: 11–29.

Casulli, V. and E. Cattani, 1994. Stability, accuracy and efficiency of a semi-implicit method for three-dimensional shallow water flow. Computers Math. Applic. 27: 99–112.

Gaillard, J., 1981. A predictive model for water quality in reservoirs and its application to selective withdrawal. PhD thesis, Colorado State University, Fort Collins, Colorado.

Gargett, A.E., 1991. Physical processes and the maintenance of nutrientrich euphotic zones. Limnology and Oceanography 36: 1527–1545.

Garnier, J., 1984. Evolution de la transparence et de la concentration en chlorophylle a des eaux d'une sablière (lac de Créteil, région parisienne) au cours de quatre années (1979, 1982). Revue Française des Sciences de l'Eau 3: 71–81.

Gaspar, P., Y. Grégoris and J.-M. Lefevre, 1990. A simple eddy kinetic model for simulations of the oceanic vertical mixing: Tests at Station Papa and long-term upper ocean study site. J. Geophys. Res. 95: 16179–16193.

Giovanoli, F., 1990. Horizontal transport and sedimentation by interflows and turbidity currents in Lake Geneva. In: Tilzer, M. and C. Serruya (ed.), Springer-Verlag: Large Lakes, pp. 175–195.

Goudsmit, G.-H., P. Reichert and A. Wüest, 1996. Modelling of physical and bio-geochemical properties in lakes using AQUASIM. In: Hydroinformatics '96. Müller. Balkema, Rotterdam. ISBN 90 5410 8525.

Hamilton, D.P., G.C. Hocking and J. Patterson, 1995. Criteria for selection of spatial dimensionality in the application of one and two dimensional water quality models. In: Modsim95, Univ. of. Newcastle (ed.), Int. Congress on Modelling and Simulation. Vol 3: Water Ressources and Ecology.

Hamilton, D.P. and S.G. Schladow, 1997. Prediction of water quality in lakes and reservoirs. Part I – model description. Ecological Modelling 96: 91–110.

Henderson-Sellers, B., 1984. Engineering Limnology. Pitman Advanced Publishing Program, London, 356 pp.

Holloway, G., 1984. Effects of velocity fluctuations on vertical distributions of phytoplankton. Journal of Marine Res. 42: 559–571.

Huber, W. and D. Harleman, 1968. Laboratory and analytical studies of thermal stratification in reservoirs. Technical report, Massachussetts Institute of Technology, Cambridge Mass.

Imberger, J. and J.C. Patterson, 1981. A dynamic reservoir simulation model-DYRESM: 5. In: H.B. Fischer (ed.), Academic Press, California, USA: Transport models for inland and coastal waters, pp. 310–360.

Imberger, J. and J.C. Patterson, 1990. Physical limnology. Advances in Applied Mechanics 27: 303–477.

Jassby, A. and T. Powell, 1975. Vertical patterns of eddy diffusion during stratification in Castle Lake, California. Limnology and Oceanography 20: 531–543.

Kantha, L. and C. Clayson, 1994. An improved mixed layer model for geophysical applications. J. Geophys. Res. 99: 25235–25266.

Karagounis, I., J. Trösch and F. Zamboni, 1993. A coupled physical-biochemical lake model for forecasting water quality. Aquatic Sciences 55: 87–102.

Lafforgue, M., 1990. Modélisation du fonctionnement d'un écosystème lacustre: le lac d'Aydat. PhD thesis, Ecole des Mines de Paris.

Leonard, B., 1979. A stable accurate convective modeling procedure based on quadratic upstream interpolation. Computer methods in applied mechanics and engineering 19: 59–98.

MacIntyre, S., 1993. Vertical mixing in a shallow, eutrophic lake: Possible consequences for light climate of phytoplankton. Limnology and Oceanography 38: 798–817.

Octavio, K., G. Jirka and D. Harleman, 1977. Vertical heat transport mechanisms in lakes and reservoirs. Technical Report 227, Department of Civil Engineering, M.I.T.

Patterson, J.C., 1991. Modelling the effects of motion on primary production in the mixed layer of lakes. Aquatic Sciences 53: 219–238.

Queney, P., 1974. Eléments de météorologie. Masson, Paris, 300 pp.
Reichert, P., 1994. AQUASIM – a tool for simulation and data analysis of aquatic systems. Wat. Sci. Tech. 30: 21–30.
Riley, M.J. and G.S. Heinz, 1988. MINLAKE: a dynamic lake water quality simulation model. Ecological Modelling 43: 155–182.
Ryan, P. and D. Harleman, 1971. Prediction of the annual cycle of temperature changes in a stratified lake or reservoir: mathematical model and user's manual. Technical Report 137, Massachussetts Institute of Technology.
Simons, T., 1981. The seasonal climate of upper ocean: data analysis and model development, interim report. Technical report, National Water Research Institute, Ontario, Canada.
Smith, I., 1979. Hydraulic conditions in isothermal lake. Freshwater Biology 9: 119–145.
Tassin, B., 1986. Contribution à la modélisation du lac Léman, modèles physiques et biogéochimiques. PhD thesis, Ecole Nationale des Ponts et Chaussées, Paris.
TVA 1972. Heat and mass transfer between a water surface and the atmosphere. Technical report 14 (0-6803), TVA Water Ressources Research, Norris, Tennessee.
Vinçon-Leite, B., 1991. Contribution de la modélisation mathématique à l'étude de la qualité de l'eau dans les lacs sub-alpins: le lac du Bourget (Savoie). PhD thesis, École Nationale des Ponts et Chaussées, Paris.

Received 14 January 1998;
revised manuscript accepted 7 October 1999.